

VITA

Name-Surname	Mr. Worawut Makcharoen
Date of birth	9 June 1981
Province	Samutsakhon
Education	M.Sc. (Materials), Chiang Mai University, Chiang Mai (2005)
Scholarship	Ph.D. Scholarship from Development and Promotion of Science and Technology Talents Project (DPST)

Conference and Publications

National Conference:

1. Worawut Makcharoen, Jerapong Tontrakoon, Gobwute Rujijanagul and Tawee Tunkasiri, Effect of Zirconium Substitution on the Dielectric Properties of $\text{CaCu}_3\text{Ti}_4\text{O}_{12}$ Ceramics Prepared via Vibro-Milling Method, *The 28th Annual Conference of the Microscopy Society of Thailand*, Mae Fah Luang University, Chiang rai, Thailand, 5 – 7 January (2011).

International Conference:

1. **Worawut Makcharoen**, Jerapong Tontrakoon, Prasak Thavornnyutikarn, David P. Cann and Tawee Tunkasiri, “Dielectric properties and Microstructure of $\text{CaCu}_3\text{Ti}_{4-x}\text{Mn}_x\text{O}_{12}$ ceramics”, *IEEE International Symposium on the Applications of Ferroelectrics (ISAF 2008 Conference)*, Santa Fe, New Mexico, USA, 24-27 February 2008.
2. **Worawut Makcharoen**, Jerapong Tontrakoon, Prasak Thavornnyutikarn and Tawee Tunkasiri, “Effects of the microstructure and dielectric properties on Mn doped $\text{CaCu}_3\text{Ti}_4\text{O}_{12}$ ceramics”, *International Conference on Smart Materials-Smart/Intelligent Materials and Nano Technology & 2nd International Workshop on Functional Materials and Nanomaterials (SmartMat-'08 & IWOFM-2)*, The Imperial Mae Ping Hotel, Chiang Mai, Thailand, 22-25 April 2008.
3. **Worawut Makcharoen**, Jerapong Tontrakoon, Prasak Thavornnyutikarn and Tawee Tunkasiri, Dielectric Properties of $\text{CaCu}_3\text{Ti}_{4-x}\text{Mn}_x\text{O}_{12}$ Ceramics, *The Advance Materials and Nanotechnology (AMN4 Conference)*, University of Otago, New Zealand, 8-12 February 2009.
4. **Worawut Makcharoen**, Jerapong Tontrakoon, Gobwute Rujijanagul and Tawee Tunkasiri, The Effect of In_2O_3 doping on the dielectric properties of $\text{CaCu}_3\text{Ti}_4\text{O}_{12}$ ceramics, *The 10th Russia/CIS/Baltic/Japan Symposium on Ferroelectricity (RCBJSF-10)*, Yokohama, Japan, 20-24 June, 2010.

5. **Worawut Makcharoen**, Jerapong Tontrakoon, Gobwute Rujijanagul and Tawee Tunkasiri, The Effect of GeO_2 doping on the dielectric properties of $\text{CaCu}_3\text{Ti}_4\text{O}_{12}$ ceramics, *The 10th Russia/CIS/Baltic/Japan Symposium on Ferroelectricity (RCBJSF-10)*, Yokohama, Japan, 20-24 June, 2010.
6. **Worawut Makcharoen**, Jerapong Tontrakoon, Gobwute Rujijanagul and Tawee Tunkasiri, Dielectric properties of Cs_2CO_3 dope CCTO ceramics, *The 7th Asian Meeting on Ferroelectricity and The 7th Asian Meeting on Electroceramics (AMF-AMEC-2010)*, Jeju Island, Korea, 28 June – 1 July, 2010.
7. **Worawut Makcharoen**, Jerapong Tontrakoon, Gobwute Rujijanagul and Tawee Tunkasiri, Effect of indium and cerium substitution on the dielectric properties of $\text{CaCu}_3\text{Ti}_4\text{O}_{12}$ ceramics, *The 7th Asian Meeting on Ferroelectricity and The 7th Asian Meeting on Electroceramics (AMF-AMEC-2010)*, Jeju Island, Korea, 28 June – 1 July, 2010.

International Publications:

1. **Worawut Makcharoen**, Jerapong Tontrakoon, Prasak Thavornytikarn, David P. Cann and Tawee Tunkasiri, “Dielectric properties and microstructure of $\text{CaCu}_3\text{Ti}_{4-x}\text{Mn}_x\text{O}_{12}$ ceramics”, *Applications of Ferroelectrics*, 2008. ISAF 2008. 17th IEEE International Symposium on the Applications of Ferroelectrics, 1 No.4693905.

2. **Worawut Makcharoen**, Jerapong Tontrakoon, Prasak Thavornyutikarn and Tawee Tunkasiri, “Dielectric properties of $\text{CaCu}_3\text{Ti}_{4-x}\text{Mn}_x\text{O}_{12}$ ceramics”, *AIP Conference Proceedings*, 25, (2009) 1151 p. 9-12.
3. **Worawut Makcharoen**, Jerapong Tontrakoon, Gobwute Rujijanagul and Tawee Tunkasiri, “The effect of GeO_2 and In_2O_3 doping on the dielectric properties of $\text{CaCu}_3\text{Ti}_4\text{O}_{12}$ ceramics prepared via vibro-milling method”, Submitted to *Ferroelectric*.
4. **Worawut Makcharoen**, Jerapong Tontrakoon, Gobwute Rujijanagul and Tawee Tunkasiri, “Effect of Zirconium Substitution on the Dielectric Properties of $\text{CaCu}_3\text{Ti}_4\text{O}_{12}$ Ceramics Prepared via Vibro-Milling Method”, *Proceeding of the 28th Annual Conference of the Microscopy Society of Thailand*, January 2011.
5. **Worawut Makcharoen**, Jerapong Tontrakoon, Gobwute Rujijanagul and Tawee Tunkasiri, “Effect of Cesium and Cerium Substitution on the Dielectric Properties of $\text{CaCu}_3\text{Ti}_4\text{O}_{12}$ Ceramics”, *Ceramics International*, pending acceptance.

Dielectric properties of $\text{CaCu}_3\text{Ti}_{4-x}\text{Mn}_x\text{O}_{12}$ ceramics

W. Makcharoen, J. Tontrakoon, P. Thavornnyutikarn*, T. Tunkasiri

Department of Physics, Faculty of Science, Chiang Mai University, Chiang Mai 50200, Thailand.

* Department of Chemistry, Faculty of Science, Chiang Mai University, Chiang Mai 50200, Thailand.

Abstract. In this work, we have reported the dielectric properties of the Mn doped $\text{CaCu}_3\text{Ti}_4\text{O}_{12}$ (CCTO) ceramics. The conventional solid-state reaction was employed. By the partial Mn -for Ti substitution, the dielectric loss was suppressed remarkably while the dielectric constant (ϵ_r) still remains high. The sample $\text{CaCu}_3\text{Ti}_{3.76}\text{Mn}_{0.24}\text{O}_{12}$ exhibits a high ϵ_r over 1200 and a low dielectric loss below 0.06 at room temperature. Furthermore, the ϵ_r value of this sample shows rather independent with temperature. SEM micrographs show that no impurity was observed in the Mn doped CCTO ceramics which exhibit the dense microstructures with out abnormal grains. This $\text{CaCu}_3\text{Ti}_{4-x}\text{Mn}_x\text{O}_{12}$ system is believed to be a promising candidate for capacitor applications.

Keywords: $\text{CaCu}_3\text{Ti}_4\text{O}_{12}$; CCTO; Dielectric properties; Perovskite

PACS: 82.45.Un

INTRODUCTION

The perovskite - type compound $\text{CaCu}_3\text{Ti}_4\text{O}_{12}$ (CCTO), was first synthesized by Bochu et al. [1]. This titanate oxide crystallizes in a cubic structure with $Im\bar{3}$ space group. The TiO_6 octahedra are tilted, resulting in the doubling of the perovskite-like lattice parameter and involves a square planar arrangement of the oxygen around the Cu^{2+} cations. [2,3]. The dielectric constant is almost temperature independent from 200 K to 400 K, with low frequency dielectric constant of CCTO can be as high as 95,000 in single crystals, and 12,000 in sintered pellets [2, 4]. For the ceramic [2] and thin-film [5] samples at room temperature, the typical value of $\tan \delta$ is about 0.2 at 10 kHz.

The high dielectric constant of CCTO can then be understood based on a barrier layer mechanism. This is a well-known mechanism for titanates that are processed in such a way as to produce grains that are reduced and conducting when coupled with grain boundaries that are oxidized and much less conducting [2].

The partial substitution of divalent Ca^{2+} by the trivalent La^{3+} was carried out, in order to increase the

conductivity of the grains [6]. The loss angle can be reduced by adding of some elements such as manganese oxide (MnO_2) [7]. In this work we extend the study on CCTO samples with substitutions of Ti ions by Mn ions leading to the formula $\text{CaCu}_3\text{Ti}_{4-x}\text{Mn}_x\text{O}_{12}$, ranging from $x = 0.08$ up to 0.40. Characterization of the samples was carried out using x-ray diffraction (XRD) and scanning electron microscopy (SEM). Other physical properties such as, density, dielectric constant and loss angle were intensively studied.

Experimental procedure

The $\text{CaCu}_3\text{Ti}_4\text{O}_{12}$ (CCTO) powder was prepared by the mixed-oxide route. High purity (> 99.9%) CaCO_3 (Riedel-de Haen), TiO_2 (Riedel-de Haen) and CuO (Aldrich) powders were weighed in an appropriate ratio, fully mixed by ball milling for 24 h using zirconia balls in ethanol media. After being dried, the powders were calcined at 850°C for 2 h to form the CCTO powder. In searching for the most appropriate sintering temperature, the calcined powder was granulated using polyvinyl alcohol (PVA) 3% binder and formed under a uniaxial pressure of 1500 kg/cm^2 into discs, typically 15 mm in diameter and 2 mm in thickness. The discs were sintered in air at $850 - 1050^\circ\text{C}$ in a step of 50°C (with soaking time of 2 h). The ramping and the cooling rates were 300°C/h . The XRD and density results showed that the most

appropriate sintering temperature of CCTO was 1000°C. The substituted CCTO samples was prepared by mechanically ground (24 h) mixtures of the calcined CCTO powder and various amounts of $\text{MnCl}_2 \cdot 4\text{H}_2\text{O}$ powders, leading to the formula $\text{CaCu}_3\text{Ti}_{4-x}\text{Mn}_x\text{O}_{12}$ ($x = 0.08, 0.16, 0.24, 0.32$ and 0.40). The mixtures were formed into discs employing the same process as that of the undoped samples. The discs were sintered in air at 1000°C for 2 h, with the same ramping and the cooling rates. During sintering oxygen gas was fed into the furnace at the rate of 100 c.c./min. The discs were polished to produce the flat uniform surfaces. All the samples were characterized by x-ray diffraction (JEOL JDX-8030) at room temperature using CuK_α radiation as the x-ray source. Silver paste was used as the electrical contact. The painted samples were dried at 750 °C for 20 minutes.

The polish ceramics were observed using SEM (JEOL JSM-5910LV) to study the microstructure.

The dielectric constants and loss tangents against temperature, were measured at the frequency of 1 kHz (using HP 4192A LCZ meter).

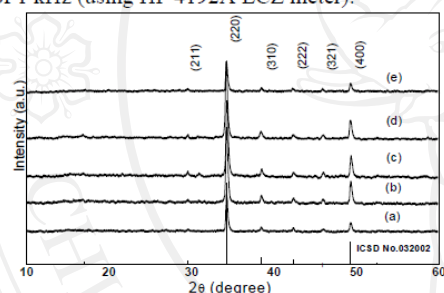


Figure 1. Powder XRD results of CCTO ceramic samples, at various sintering temperatures. (a) 850°C/2 h, (b) 900°C/2 h, (c) 950°C/2 h, (d) 1000°C/2 h, and (e) 1050°C/2 h.

Results and discussion

Figure. 1 shows the x-ray diffraction results for the CCTO ceramic samples at various temperatures. All the peaks can be attributed to CCTO, based on the data in the Inorganic Crystal Structure Database (ICSD) No.032002, having the lattice parameter (a) of 7.37 Å. It can be seen that the CCTO phase started to form at 850°C and most pronounced at

1000°C, whilst sintering at 1050°C yielded relatively lower intensity of the main peaks (220), indicating lower content of CCTO. Furthermore, the samples melted at the highest sintering temperature (1100°C). The density results of the calcined powder also showed that the highest density was obtained at 1000°C (data not shown here). This is in agreement with our XRD results and that of Yang et al.[8] and Brize et al.[9].

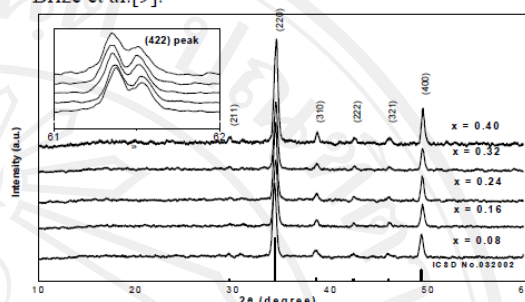


Figure 2. Powder XRD results of $\text{CaCu}_3\text{Ti}_{4-x}\text{Mn}_x\text{O}_{12}$. The top left inset is an expanded view of the XRD patterns around $2\theta = 61.4^\circ$.

The XRD results for the Mn-doped CCTO samples were presented in Figure.2. All the peaks can be well indexed using the same data base (ie.ICSD No.032002). The lattice constants and the densities of the ceramics were tabulated in Table A. The lattice constants were obtained by a least-squares fit method. They were found to slightly increase with the increasing x, indicating that Mn does enter the lattice. When $x = 0.24$ the lattice constant tends to saturate, suggesting that the Mn solubility limit at $x \sim 0.24$ (please also see Table A). The top left inset of the figure is an expanded view of the XRD pattern around $2\theta = 61.4^\circ$, showing the shift of the (422) peaks. The lower intensity peaks come from the $\text{CuK}_\alpha 2$ radiation. The increase of the lattice constant is probably due to the fact that Mn ion has larger ionic radius than Ti ion. In general, the practical frequency employed in capacitor applications is around 1 kHz, though the CCTO system is frequency dependent.

TABLE 1. Percentage of the density and the lattice parameter (a) of the Mn-doped CCTO

$\text{CaCu}_3\text{Ti}_{4-x}\text{Mn}_x\text{O}_{12}$ (x values)	Density* (%)	lattice parameter a (Å)
0	94.05	7.370
0.08	93.17	7.396
0.16	92.85	7.398
0.24	91.77	7.403
0.32	91.65	7.403
0.40	90.96	7.403

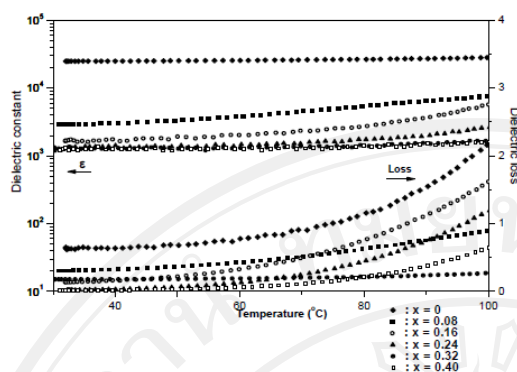


Figure 3. Temperature dependence of the dielectric constant and loss tangent for the $\text{CaCu}_3\text{Ti}_{4-x}\text{Mn}_x\text{O}_{12}$ sample, sintered at $1000^\circ\text{C}/2\text{h}$ and measured at frequency 1 kHz.

Figure 3, shows the dielectric constant and dielectric loss of Mn doped CCTO, against the temperature ranging from room temperature to 100°C . As can be seen, at the room temperature, the dielectric constant (ϵ_r) decreases from 15000, with the increasing x and ϵ_r tends to be stable (about 1200) when $x \geq 0.24$. This trend agrees well with the lattice constant results in Figure. 2 (please also see at Table A). Besides, the ϵ_r is rather constant with the temperature. The dielectric loss ($\tan\delta$) does decrease with the increasing x as generally expected. The highest and lowest values were 0.7 (for $x=0$) and 0.06 (for $x=0.24$), respectively (at room temperature). This is slightly below that obtained by Feng et al.[6] who worked on La doped CCTO system. The decrease of ϵ_r and $\tan\delta$ may be due to the fact that during sintering there was a supply of oxygen gas in the system. Similar result was also observed by Schmid and Mader [10]. Thus there is a probability that Mn^{2+} (from $\text{MnCl}_2 \cdot 4\text{H}_2\text{O}$) could be oxidized to Mn^{4+} and could substitute the Ti^{4+} lattice site, leading to the formula of $\text{CaCu}_3\text{Ti}_{4-x}\text{Mn}_x\text{O}_{12}$. This may cause the reducing of Ti vacancies, and therefore the conductivity of the ceramic decreases. However, the oxidation of Mn^{2+} to Mn^{3+} also could not be neglected. Mn^{3+} can behave as acceptors for electrons liberated from oxygen vacancy traps and thus prevent them from entering the conduction band. Nevertheless, at $x=0.24$, the $\tan\delta$ increased up to 1 against that of undoped (~ 2) at 100°C . Figure. 4 shows the SEM micrographs of the crack surface of Mn doped CCTO samples sintered at 1000°C . As can be seen that the undoped sample (Figure. 4 A), the grain size of the CCTO sample was quite high ($\sim 10\mu\text{m}$) with small pores scattered around the grains. This may be due to melting and abnormal grain growth. Similar result was also observed by Mohamed et al. [11]. However, the dielectric constant of CCTO ceramics was higher than that of CCTO ceramics sintered at 1035°C for 3h as

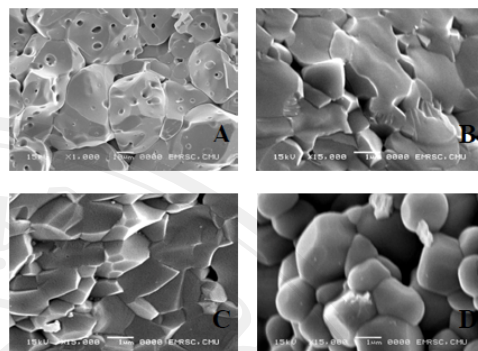


Figure 4. SEM pictures of the crack of $\text{CaCu}_3\text{Ti}_{4-x}\text{Mn}_x\text{O}_{12}$ sintering at 1000°C for 2 h. Samples A: $x=0$, B: $x=0.08$, C: $x=0.24$, and D: $x=0.40$.

revealed by Fang and Shiau [12]. Microstructural analysis also revealed that the grain size of the samples produced notable decrease, as measured by the lines intercept method, decreased from $\sim 10\mu\text{m}$ for undoped sample to $\sim 2.5\mu\text{m}$ for $\text{CaCu}_3\text{Ti}_{3.76}\text{Mn}_{0.24}\text{O}_{12}$ sample (Figure. 4. B and C). However, at $x=0.40$ (Figure. 4. D) pores were seen around the grains and this may affect the reducing of the dielectric constant.

Conclusions

The effects of Mn doped on the dielectric constant (ϵ_r), dielectric loss ($\tan\delta$) of $\text{CaCu}_3\text{Ti}_{4-x}\text{Mn}_x\text{O}_{12}$ ($x=0, 0.08, 0.16, 0.24, 0.32$ and 0.40) were examined. Dielectric constant and dielectric loss (at 1 kHz) were investigated at room temperature and 100°C . For $x=0.24$ sample, the $\tan\delta$ was found to increase from 0.06 (at room temperature) to 1 (at 100°C). The dielectric constant of this sample remained high (~ 1200) and rather independent with temperature. The microstructure of the cracked surface of Mn doped CCTO samples sintered at 1000°C , appeared dense. The calculated densities of the ceramics were rather high (above 90% of the theoretical density).

Acknowledgments

The authors would express their sincere thanks to the Thailand Research Funds (TRF) of Thailand and the Graduate School, Chiang Mai University. For their support.

REFERENCES

1. B. Bochu, M.N. Deschizeaux, J.C. Joubert, A. Collomb, J. Chenavas, M. Marezio, J. Solid State Chem. 29 (1979) 291–298.
2. M.A. Subramanian, D. Li, N. Duan, B.A. Reisner, A.W. Sleight, J. Solid State Chem. 151 (2000) 323–325.
3. M. Sandra, Moussa, J. Brendan, Kennedy, Pergamon Mater. Res. Bull. 36 (2001) 2525–2529.
4. Y. Lin, Y.B. Chen, T. Garret, S.W. Liu, C.L. Chen, L. Chen, R.P. Bontchev, A. Jacobson, J.C. Jiang, E.I. Meletis, J. Horwitz, H.D. Wu, Appl. Phys. Lett. 81 (2002) 631.
5. W. Si, E. M. Cruz, P. D. Johnson, P. W. Barnes, P. Woodward, and A. P. Ramirez, Appl. Phys. Lett. 81, 2056 (2002).
6. Lixin Feng, Xiaoming Tang, Yueyue Yan, Xuezhai Chen, Zhengkuan Jiao, and Guanghan Cao. phys. stat. sol. (a) 203, No. 4, R22–R24 (2006).
7. Buchanan R.C 1986 Ceramics materials for electronics, Processing, Properties and Applications (New York:Marcel Dekker)p.110.
8. Jing Yang, Mingrong Shen, Liang Fang, Materials Letters 59 (2005) 3990 – 3993.
9. V. Briz'e, G. Gruener, J. Wolfman, K. Fatyeyeva, M. Tabellout, M. Gervais, F. Gervais, Materials Science and Engineering B 129 (2006) 135–138.
10. H.K. Schmid, W. Mader, Micron 37 (2006) 426–432.
11. Julie J. Mohamed, Sabar D. Hutagalung, M. Fadzil Ain, Karim Deraman, Zainal A. Ahmad, Materials Letters 61 (2007) 1835–1838.
12. Tsang-Tse Fang, Hsu-Kai Shiau, J. Am. Ceram. Soc., 87 [11] 2072 - 2079 (2004).

The Effect of GeO_2 and In_2O_3 Doping on the Dielectric Properties of $\text{CaCu}_3\text{Ti}_4\text{O}_{12}$ Ceramics Prepared via Vibro-Milling Method

WORAWUT MAKCHAROEN,^{1,*} JERAPONG TONTRAKOON,¹
 GOBWUTE RUJIANAGUL,¹ AND TAWEE TUNKASIRI^{1,2}

¹Department of Physics, Faculty of Science, Chiang Mai University,
 Chiang Mai 50200, Thailand

²School of science, Mae Fah Lung University, Chiang Rai 57100, Thailand

In this work, effects of GeO_2 and In_2O_3 doping on the dielectric properties of CCTO were investigated. Doping levels range from 0.5 to 2.0 mol%. The vibro-milling method was employed for processing. The dopant addition produced a slightly smaller grain size. A reduction in dielectric constant was observed, but it is still high. The 2.0 mol% GeO_2 and In_2O_3 doped samples exhibited high dielectric constant of about 25,000 and 23,000 and low dielectric loss with 0.06 and 0.05 respectively at room temperature and at 10 kHz. The dielectric measurements showed that the modified samples exhibited a strong dielectric independency of temperature and frequency. In addition, the loss tangent reduced after doping. From this results, it can be incurred that GeO_2 and In_2O_3 doping, processed via vibro-mill are the suitable methods to achieve the stability of high ϵ_r and low loss ceramics.

Keywords High dielectric material; dielectric properties; microstructure

Introduction

Recently, much attention has been paid on $\text{CaCu}_3\text{Ti}_4\text{O}_{12}$ (CCTO) due to its high dielectric constant $\epsilon_r \sim 10,000$ to 100,000 and fine thermal stability over a wide temperature ranges from 100–400 K. The dielectric properties of CCTO has a potential for important applications in microelectronics [1–3]. CCTO has a cubic perovskite like structure with a lattice parameter, $a \sim 7.393 \text{ \AA}$ [4]. It does not undergo any structural phase transition over the same temperature range. Change in dielectric constant of CCTO has been widely related to its microstructure [4]. In order to explain the origin of the high dielectric constant behavior in CCTO, many models have been proposed. The internal barrier layer capacitor (IBLC) model of Schottky barriers at the grain boundaries between semiconducting grains is widely accepted for analyzing the dielectric properties of CCTO [5, 6]. It is also reported that dielectric properties of CCTO depends on many factors such as processing and doping. There are many examples in the literature showing the effects of dopants (Zr, Fe, Co, Nb, Ni, Sc and La etc.) in CCTO -based dielectric ceramics [7–13]. Furthermore, Tsoutsou *et al.* [14] reported that dielectric constant in ZrO_2 thin film was improved by doping GeO_2 .

Received June 20, 2010; in final form July 11, 2010.

*Corresponding author. E-mail: warmak77@hotmail.com

Kwon *et al.* [15] reported that the doping of Cr_2O_3 in CCTO could increase its dielectric constant. As In ion has the same valency with Cr ion (3^+) we expected that the doping of In_2O_3 could produce similar result, even though its ionic size is larger. According to Kashcheev and Zemlyanoi [16], powder processing via vibro-milling could stimulate the grain activity. In this work, the effects of GeO_2 and In_2O_3 doping on CCTO ceramics were studied, with the expectation that both Ge and In ions would go into B-site of CCTO and that they could improve their dielectric properties. The CCTO ceramics were fabricated via a solid-state reaction. The vibro-mill was employed to produce CCTO powder. Properties of the obtained ceramics were investigated with the aim of improving its dielectric characteristics. Characterization of the samples was carried out using x-ray diffraction (XRD) and scanning electron microscopy (SEM). Physical properties such as, density, dielectric constant and loss tangent were also investigated.

Experimental

The unmodified $\text{CaCu}_3\text{Ti}_4\text{O}_{12}$ (CCTO) powder was prepared by the mixed-oxide route. High purity ($> 99.9\%$) CaCO_3 (Riedel-de Haen), TiO_2 (Riedel-de Haen) and CuO (Aldrich) powders were weighed in the desired ratio, fully mixed by yttria-stabilized zirconia balls in ethanol media and milled using a vibratory mill for 6 h. After being dried, the powders were calcined at 900°C for 2 h to form the CCTO powder. The calcined powder was granulated using polyvinyl alcohol (PVA) 3% binder and formed under a uniaxial pressure of $2,000 \text{ kg/cm}^2$ into discs, typically 10 mm in diameter and 2 mm in thickness. The discs were sintered in air at $1,100^\circ\text{C}$ in a step of 5°C/min (with soaking time of 4 h). For the doping study, GeO_2 and In_2O_3 powders at various concentrations (0.5, 1.0 and 2.0 mol%) were mixed to CCTO at the calcination stage. The mixtures were formed into discs employing the same process as that of the unmodified samples. The discs were sintered in air at $1,100^\circ\text{C}$ for 4 h, with the same ramping and the cooling rates. The discs were polished to produce the flat uniform surfaces. All the samples were characterized by an x-ray diffractometer (Bruker D8 Discover) at room temperature using Cu K_α radiation. Silver paste was used as the electrical contact. The painted samples were dried at 750°C for 20 minutes. The fracture surfaces of ceramics were observed using SEM (JEOL JSM-5910LV) to study the microstructure. The dielectric constants and loss tangents against temperature were measured at the frequency of 100 Hz–500 kHz (using an Agilent 4284A LCR meter).

Results and Discussion

The XRD patterns of GeO_2 doped CCTO ceramics are displayed in Fig. 1(a). All diffraction peaks correspond to the known peaks of the standard CCTO, indexed from the data in the Inorganic Crystal Structure Database (ICSD) file No.032002. All samples exhibited a phase-pure perovskite, no trace of impurity or raw materials peaks were observed, under the detection limit of the XRD equipment. The XRD patterns of In_2O_3 doped CCTO samples are not shown here since they are similar to that of Fig. 1(a). The crystal symmetry of the samples at room temperature was determined to be cubic. Value of lattice constant as a function of GeO_2 and In_2O_3 contents are shown in Fig. 1(b). The lattice constant of both GeO_2 and In_2O_3 doped samples show the same trend, i.e. they slightly increase with increasing the GeO_2 and In_2O_3 contents. With 2.0 mol% of GeO_2 and In_2O_3 doping, the shift in lattice parameters were 0.018%, 0.021% respectively. This may indicate that main part of dopants did not go into solid solution within the grains. This is consistent with the

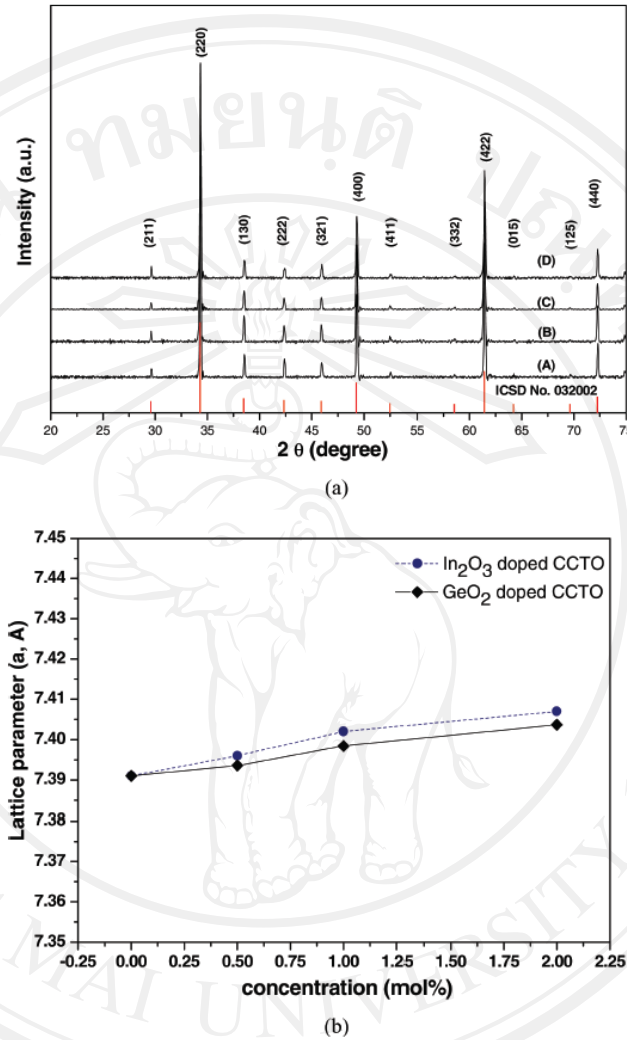


Figure 1. (a) XRD patterns pure and modified CCTO: A = 0 mol% Ge, B = 0.5 mol% Ge, C = 1 mol% Ge, and D = 2 mol% Ge. (b) lattice parameter (Å) as a function of Ge and In concentration.

increased DC resistance observed in GeO₂ and In₂O₃ – doped samples, thus could result in the decrease of the loss tangent, (as reported in the electrical results). However, the amounts of dopants may be still too low to show up in XRD data. In the relation to the internal barrier layer model, doping does not affect the grain electrical properties but rather modifies the grain boundary resistance [15]. The density and linear shrinkage slightly increased with increasing amounts of GeO₂ and In₂O₃. Plots of linear shrinkage and density as a function of GeO₂ and In₂O₃ contents are shown in Fig. 2. It can be concluded that both dopants

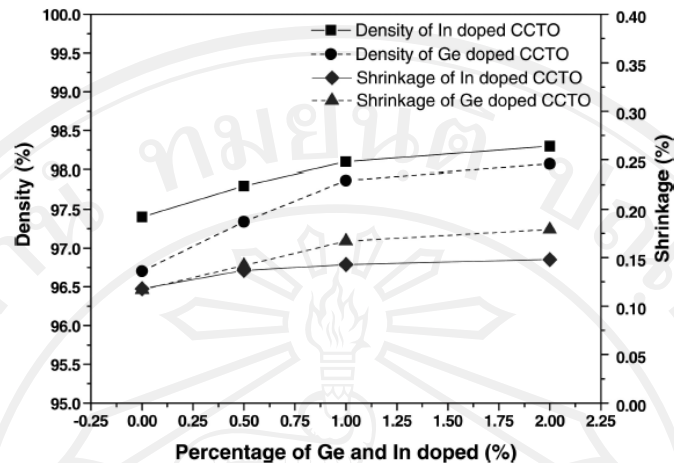


Figure 2. Density and shrinkage as a function of doping concentration of the samples.

enhance the densification of CCTO ceramics. The highest values of 2.0mol% of both GeO_2 doped CCTO and In_2O_3 doped CCTO are 4.95, 4.97 g /cm³ respectively, about 98% and 98.25% of the theoretical value of CCTO (5.053 g /cm³).

Fracture surfaces of the CCTO ceramics (undoped and doped 2.0mol% of GeO_2 and In_2O_3) are shown in Fig. 3. Partial intergranular fracture was observed for the unmodified sample. After doping, the GeO_2 doped samples exhibited a non-uniform in grain size. There was some small grains occurred between large grains. The fracture mode changed to mainly intragranular for the doped samples, suggesting a higher strengthening of the grain boundaries [17]. In contrast, the In_2O_3 doped samples showed rather smaller grains. These results indicate a rearrangement of grain boundary structure taking place due to the effect of the dopants. The decrease in grain size was observed after doping: grain size slightly decreased from 20 μm for the unmodified sample to 15 μm for the 2.0 mol% GeO_2 -doped sample. However, the grain size of the 2.0 mol% In_2O_3 -doped sample showed much smaller (2.7 μm). As observed, the grain size of GeO_2 and In_2O_3 -doped ceramics decrease with the increasing of dopants contents.

The temperature and frequency dependences of dielectric constants of undoped, GeO_2 and In_2O_3 -doped CCTO ceramics at room temperature over the frequency range of 10^2 – 10^6 Hz are illustrated in Fig. 4. The unmodified sample showed a nearly temperature-independent at high frequencies (≥ 10 kHz). Both GeO_2 and In_2O_3 2.0 mol% doped samples exhibited the same trend, i.e. decrease in the dielectric constant with the dopants contents, when compared with undoped sample. However, the dielectric constant of GeO_2 doped ceramic are still high, ~25,000, at 10 kHz, while that of In_2O_3 doped sample showed ~23,000 at 10 kHz. The dielectric constants (ϵ_r) of both GeO_2 and In_2O_3 doped samples (1.0 mol%) all showed slightly higher than that obtained from the 0.5 and 2.0 mol% doped samples, however they are in the same order. In contrast, Kwon *et al.* [15] reported the increase of dielectric constant of CCTO after doping Cr_2O_3 . They also reported that based on the internal barrier layer model, this could be explained by the enhance conductivity in grains. Figure 5 displays the loss tangents ($\tan \delta$) against temperature of the doped and undoped samples. The $\tan \delta$ values of the doped samples show lower than that of the

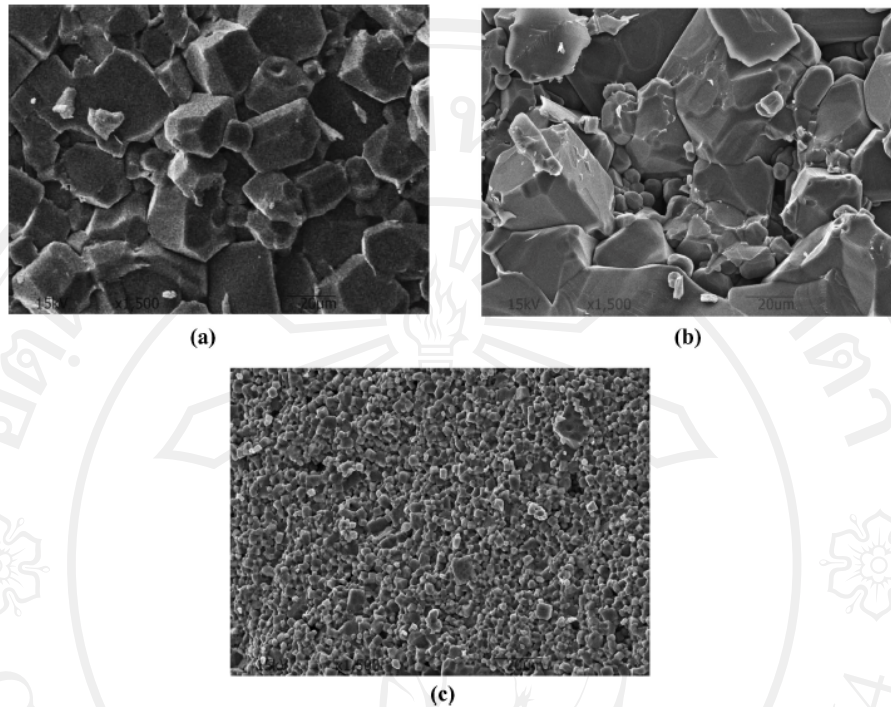


Figure 3. Fracture surfaces of selected samples: (a) pure CCTO, (b) Ge 2 mol% doped CCTO and (c) In 2.0 mol% doped CCTO.

undoped one. This is consistent with the increase of DC resistance as mentioned earlier. Both GeO₂ and In₂O₃ (2.0 mol%) doped samples show that the ϵ_r values are rather stable for all frequencies except that of low frequency (100 Hz). The $\tan \delta$ values are quite low 0.06 for GeO₂ doped sample and 0.05 for In₂O₃ doped ceramic measured at 10 kHz. The low loss tangent in doped CCTO might be due to the increase in grain boundary resistivity.

Figure 6 shows dielectric constant and loss tangent as a function of frequency at room temperature. The dielectric constant decreased with frequency, but a sharp decrease was observed at the frequencies 100 Hz to 1 kHz. The loss tangent decreased to a lower value with increasing frequency (up to 1 kHz) then increased with further frequency. A similar result was observed for the work carried out by Kwon *et al.* [15].

In this work characteristic of the grain boundary may be responsible for the effects on the increased dielectric loss of the samples. The change of the fracture mode suggested a change in grain boundary properties. It is believed that the GeO₂ and In₂O₃ addition produced an increase in total resistance of the grain boundary [15]. This may cause a reduction in conductivity as a result of lower loss tangent. Furthermore, the reduction in grain size can be associated with the decrease in dielectric constant [18, 19]. Therefore, the decrease in grain size may be related to for the reduction of the dielectric constant to some extent. From Fig. 3, it should be noted that there were some cluster of small grains placed between the large gains. These features may also have some effect on the dielectric properties. However, details on the dielectric properties in terms of the microstructure should be intensively investigated.

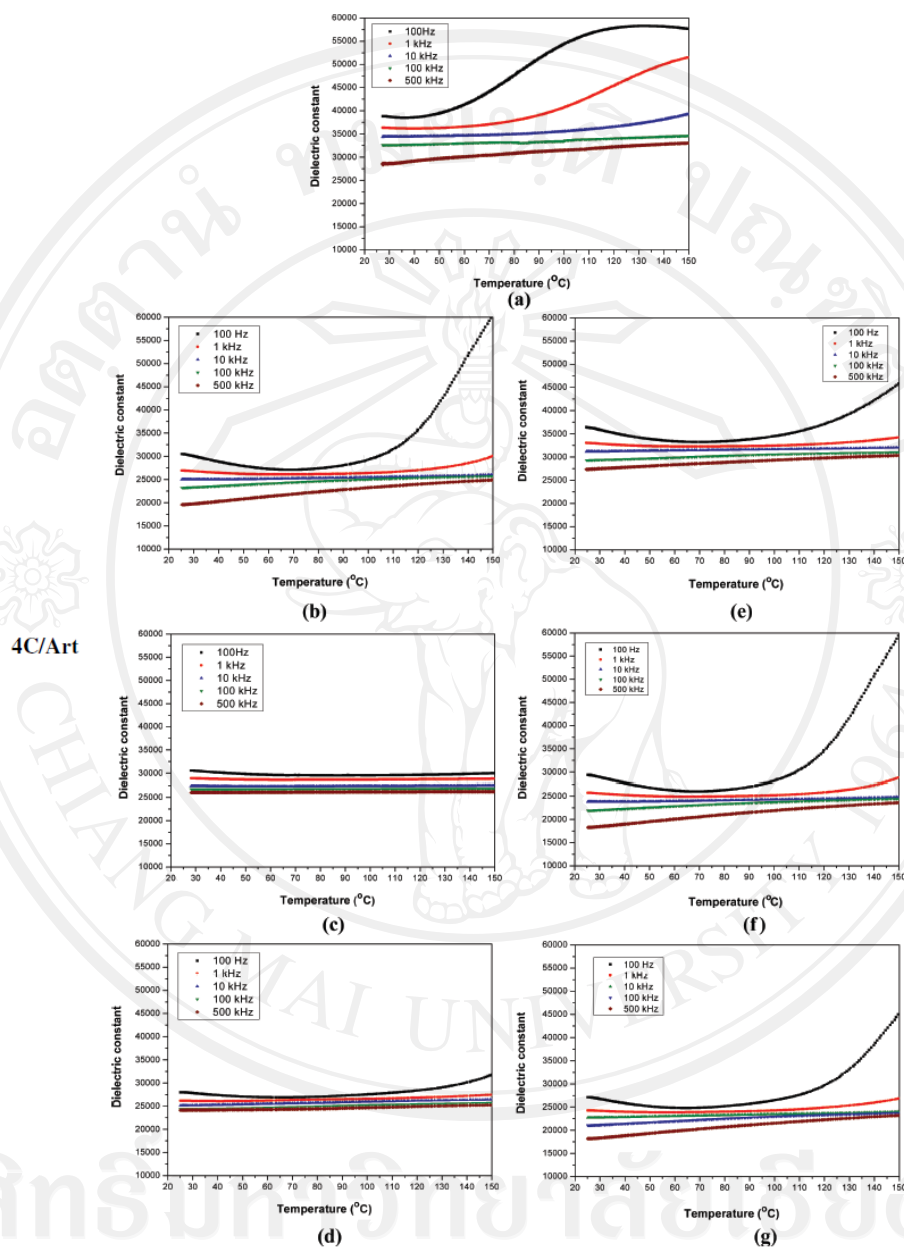


Figure 4. Dielectric constant as a function temperature of the samples: (a) undoped CCTO, (b) 0.5 mol% Ge doped CCTO, (c) 1.0 mol% Ge doped CCTO, (d) 2.0 mol% Ge doped CCTO, (e) 0.5 mol% In doped CCTO, (f) 1.0 mol% In doped CCTO and (g) 2.0 mol% In doped CCTO.

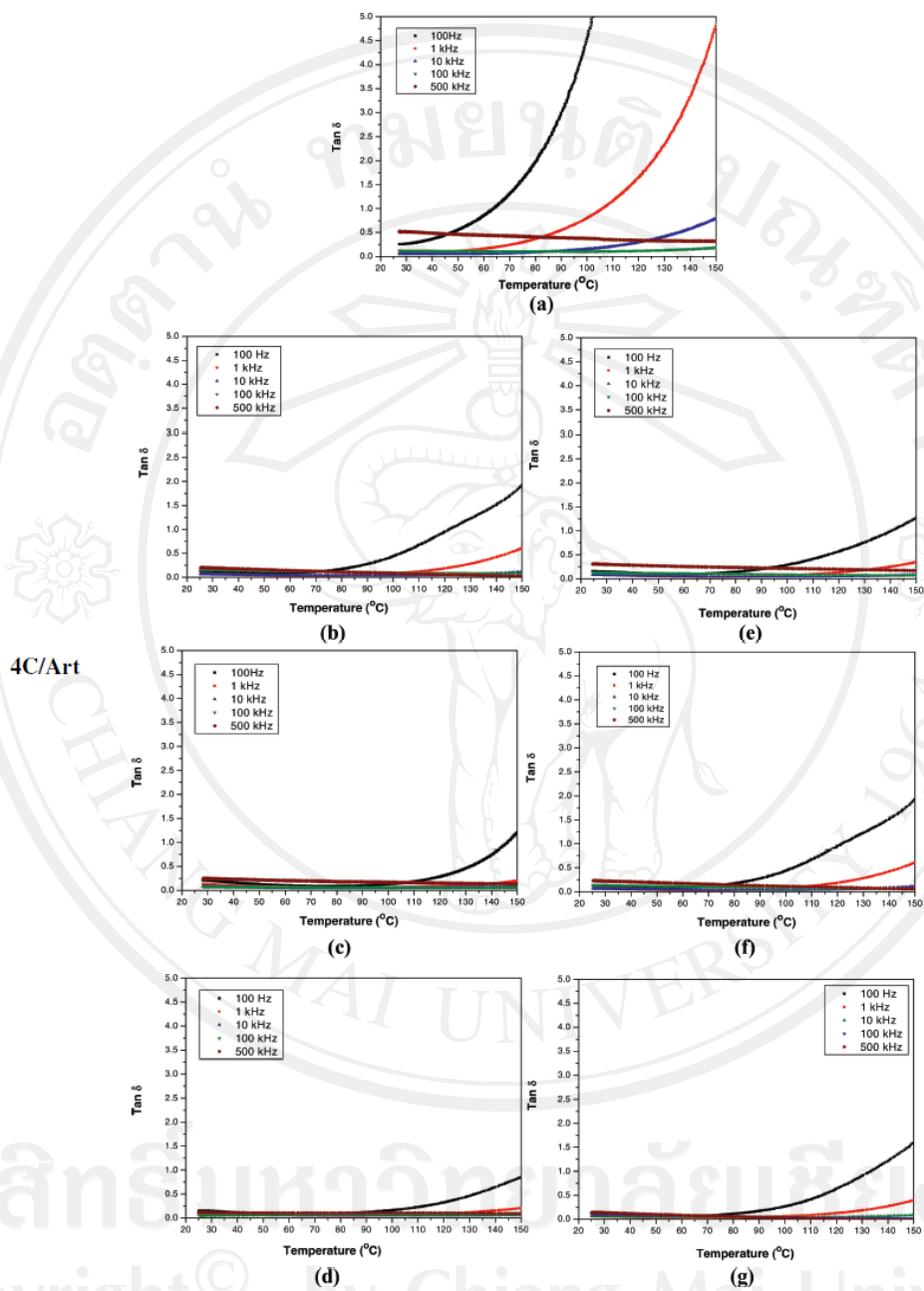


Figure 5. Tangent as a function temperature of the samples: (a) undoped CCTO, (b) 0.5 mol% Ge doped CCTO, (c) 1.0 mol% Ge doped CCTO, (d) 2.0 mol% Ge doped CCTO, (e) 0.5 mol% In doped CCTO, (f) 1.0 mol% In doped CCTO and (g) 2.0 mol% In doped CCTO.

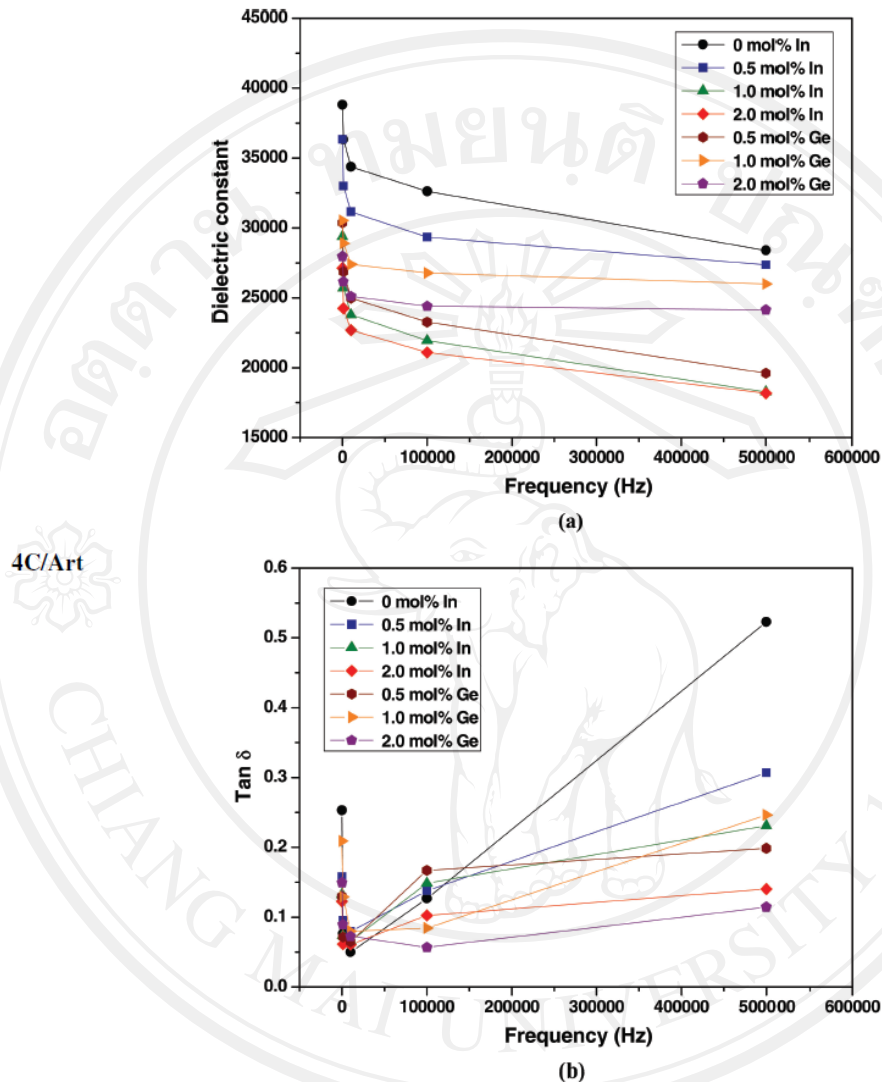


Figure 6. Dielectric properties of the samples as a function of frequency: (a) dielectric constant and (b) loss tangent.

138 Conclusions

139 The dielectric properties of GeO_2 and In_2O_3 doped CCTO (processed via vibro-milling
 140 method) were reported in this work for the first time. From the results of dielectric mea-
 141 surement at 2.0 mol% GeO_2 showed low $\tan \delta$ around 0.05 between 100 Hz–500 kHz.
 142 For the In_2O_3 (2.0 mol%) doped samples showed slightly higher. The doping produced
 143 slightly lower of the dielectric constant than that of undoped one. However, the doping

improved the temperature and frequency stability of the dielectric properties. Considering the temperature and frequency independence of the ϵ_r and $\tan \delta$ of both GeO₂ and In₂O₃ doped samples may be suitable for high ϵ_r applications.

Acknowledgments

This work was supported by Development and Promotion of Science and Technology Talents Project (DPST), Thailand, Faculty of Science and Graduate School Chiang Mai University, the Thailand Research Fund (TRF), and Office of the Higher Education Commission (OHEC).

References

1. A. P. Ramirez, M. A. Subramanian, M. Gardel, G. Blumberg, D. Li, T. Vogt, and S. M. Shapiro, *Solid State Commun.* **115**, 217–220 (2000).
2. M. A. Subramanian, D. Li, N. Duan, B. A. Reisner, and A. W. Sleight, *J. Solid State Chem.* **151**, 323 (2000).
3. C. C. Homes, T. Vogt, S. M. Shapiro, S. Wakimoto, and, A. P. Ramirez, *Science*. **293** 673–676 (2001).
4. Y. Lin, Y. B. Chen, T. Garret, S. W. Liu, C. L. Chen, L. Chen, R. P. Bontchev, A. Jacobson, J. C. Jiang, E. I. Meletis, J. Horwitz, and H. D. Wu, *Appl. Phys. Lett.* **81**, 631 (2002).
5. D. C. Sinclair, T. B. Adams, F. D. Morrison, and A. R. West, *Appl. Phys. Lett.* **80**, 2153 (2002).
6. T. B. Adams, D. C. Sinclair, and A. R. West, *Adv. Mater.* **14**, 1321 (2002).
7. G. Chiodelli, V. Massarotti, D. Capsoni, M. Bini, C. B. Azzoni, M. C. Mozzati, and P. Lupotto, *Solid State Commun.* **132**, 241 (2004).
8. D. Capsoni, M. Bini, V. Massarotti, G. Chiodelli, M. C. Mozzati, and C. B. Azzoni, *J. Solid State Chem.* **177**, 4494 (2004).
9. L. Feng, X. Tang, Y. Yan, X. Chen, Z. Jiao, and G. Cao, *Phys. Stat. Sol. A*. **203**, R22–24 (2006).
10. B. S. Prakash and K. B. R. Varma, *J. Mater. Sci. Mater. Electron.* **17**, 899 (2006).
11. W. Kobayashi and I. Terasaki, *Physica B*. **771**, 329–333 (2003).
12. M. Li, A. Feteira, D. C. Sinclair, and A. R. West, *Appl. Phys. Lett.* **88**, 232903 (2006).
13. E. A. Patterson, S. Kwon, C.-C. Huang, and D. P. Cann, *Appl. Phys. Lett.* **87**, 182911 (2005).
14. D. Tsoutsou, G. Apostolopoulos, S. Galata, P. Tsipas, A. Sotiropoulos, G. Mavrou, Y. Panayiotatos, and A. Dimoulas, *Microelectronic Engineering*. **86**, 1626–1628 (2009).
15. S. Kwon, C.-C. Huang, E. A. Patterson, and D. P. Cann, *Materials Letters*. **62**, 633–636 (2008).
16. I. D. Kashcheev and K. G. Zemlyanoi, *Refraction and Industrial Ceramics*. **46**, 1 (2005).
17. C. Punchmark, S. Jiansirisomboon, G. Rujijanagul, T. P. Comyn, Jing Yan He, and S. J. Milne, *Materials Research Bulletin*. **42**, 1269–1277 (2007).
18. B. Barbier, C. Combettes, S. Guillemet-Fritsch, T. Chartier, F. Rossignol, A. Rumeaud, T. Lebey, and E. Dutarde, *Journal of the European Ceramic Society*. **29**, 731–735 (2009).
19. A. R. West, T. B. Adams, F. D. Morrison, and D. C. Sinclair, *Journal of the European Ceramic Society*. **24**, 1439–1448 (2004).

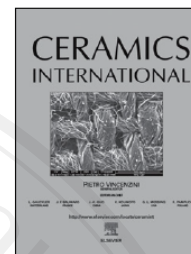
Accepted Manuscript

Title: Effect of cesium and cerium substitution on the dielectric properties of $\text{CaCu}_3\text{Ti}_4\text{O}_{12}$ ceramics

Authors: Worawut Makcharoen, Jerapong Tontrakoon, Gobwute Rujijanagul, David P. Cann, Tawee Tunkasiri

PII: S0272-8842(11)00278-1
 DOI: doi:10.1016/j.ceramint.2011.04.051
 Reference: CERI 4163

To appear in: *Ceramics International*



Please cite this article as: W. Makcharoen, J. Tontrakoon, G. Rujijanagul, D.P. Cann, T. Tunkasiri, Effect of cesium and cerium substitution on the dielectric properties of $\text{CaCu}_3\text{Ti}_4\text{O}_{12}$ ceramics, *Ceramics International* (2010), doi:10.1016/j.ceramint.2011.04.051

This is a PDF file of an unedited manuscript that has been accepted for publication. As a service to our customers we are providing this early version of the manuscript. The manuscript will undergo copyediting, typesetting, and review of the resulting proof before it is published in its final form. Please note that during the production process errors may be discovered which could affect the content, and all legal disclaimers that apply to the journal pertain.

Effect of cesium and cerium substitution on the dielectric properties of $\text{CaCu}_3\text{Ti}_4\text{O}_{12}$ ceramics

Worawut Makcharoen^a, Jerapong Tontrakoon^a, Gobwute Rujijanagul^{a, b, *}, David P. Cann^c,

Tawee Tunkasiri^{a, d}

^a*Department of Physics and Materials Science, Chiang Mai University, Thailand, 50200*

^b*Materials Science Research Center, Chiang Mai University, Thailand, 50200*

^c*Faculty of Materials Science, Department of Mechanical Engineering, Oregon State University, Corvallis, Oregon 97331-8569, USA*

^d*School of Science, Mae Fah Luang University, Chiang Rai, Thailand, 57100*

Abstract

In this study, $\text{CaCu}_3\text{Ti}_4\text{O}_{12}$ (CCTO) ceramics were doped with cesium and cerium atoms to possibly improve the electrical properties of these widely used ceramics. In all cases, pure phase perovskites were produced where cesium doping enhanced the grain growth and cerium doping produced grain growth inhibition. The cesium doping showed an improvement in loss tangent performance, in contrast to the cerium doping which showed a negative result. A high dielectric constant $> 15,000$ with a dielectric loss lower than 0.06 was observed for cesium 2.0 mol% doped at high frequencies. These results were related to the change in microstructure and the properties of grain boundary after doping.

Keywords: C. Dielectric properties; D. Perovskites; E. Capacitors; A. Grain growth

*Corresponding author. Tel.: +66 53 943376; Fax: +66 53 357512.

E-mail address: rujijanagul@yahoo.com (G. Rujijanagul)

Copyright © by Chiang Mai University
All rights reserved

1. Introduction

The high-K ceramic $\text{CaCu}_3\text{Ti}_4\text{O}_{12}$ (CCTO) first discovered by Subramanian *et al.* [1] exhibits a high dielectric constant over 10,000 at room temperature with temperature independence over the temperature range of ~ 100 -400 K [2]. For ceramic and thin-film samples at room temperature, typical values of the loss tangent are about 0.2 at 10 kHz [1,3]. The crystal lattice structure of this ceramic is composed of titanate oxide crystals arranged in a cubic structure with an $\text{Im}\bar{3}$ space group. Since the TiO_6 octahedra are tilted, there is a doubling of the perovskite-like lattice parameter which creates a square planar arrangement of the oxygen around the Cu^{2+} cations [4]. Due to these unusual properties, CCTO ceramics have an electrically heterogeneous structure with mobile charged species which show a Maxwell-Wagner relaxation behavior [5]. The internal interfaces in the polycrystalline CCTO also give rise to a polarization of the semiconducting grains and insulating grain boundaries based on the internal barrier layer capacitor (IBLC) model [6-8]. There have been numerous reports of cation substitution on the CCTO lattice structure (substitution of Co, Zr, Fe, Ni, Sc and Nb on the B-site, and substitution of La on the A-site) [8-11]. In this report, we studied cations substitution on at both the A-site and B-site of CCTO by doping cesium (Cs) and cerium (Ce). Properties of the samples were investigated and reported.

2. Experimental

The $\text{CaCu}_3\text{Ti}_4\text{O}_{12}$ powders were prepared via a conventional solid state method. For the doping Ce and Cs studies, CeO_2 and Cs_2CO_3 powders were added to CCTO powder at the calcination stage in concentrations of 1.0 and 2.0 mol%. The samples were calcined at 900°C for 2 h and sintered in air at 1100°C for 4 h. Phase formation of the samples was investigated

via an X-ray diffraction technique (XRD). The lattice parameter was calculated from the positions of the (220) and (422) X-ray diffraction peaks. Density of the ceramic samples was measured using the Archimedes method. Microstructure of the ceramics was characterized using an SEM (JEOL JSM-5910LV). Average grain sizes of the samples were determined by the intercept count method of ASTM E112, which is based on the number of the grain boundary intersections per unit length [8]. The dielectric constant and the loss tangent were measured with an Agilent 4284A LCR meter.

3. Results and discussion

Fig.1 illustrates the XRD patterns of CCTO doped with Cs and Ce, which are similar to that of many previous works [3-7]. All samples exhibited a pure perovskite phase with cubic and no symmetry no contaminating of raw materials or trace of Cs or Ce oxides. The increase in the mole fraction of Cs and Ce show no evidence of a change in symmetry in the doped ceramics. For the Cs doped samples, the XRD peaks shifted to low angles with increasing Cs concentrations (inset (a) of Fig 1). This result suggests that Cs doping produced a change in lattice parameter (a). Values of the lattice parameter of the Cs doped samples are shown in Fig.2, where it increased with increasing Cs concentrations. This indicates that the Cs^{1+} entered into the lattice of CCTO. Comparing the radius of Cs^{1+} ($r_{\text{Cs}^{1+}} = 1.69 \text{ \AA}$) to Ca^{2+} ($r_{\text{Ca}^{2+}} = 1.34 \text{ \AA}$) and Cu^{2+} ($r_{\text{Cu}^{2+}} = 0.57 \text{ \AA}$), the Cs^{1+} ions produce a larger lattice spacing as a substitute to Cu^{2+} . Thus, the increase in lattice parameter for the Cs doped samples (or the XRD peaks shifted in inset (a) of Fig.1 is the result of substituting Ca^{2+} with Cs^{1+} [9, 10]. For the Ce doping, the valance states of this ion are +3 and +4 with ionic radii of 1.06 and 0.97 \AA , respectively. Since the ionic radii for Ca and Ti sites are 1.34 and 0.68 \AA , respectively, and the lattice parameter for the Ce doped samples remained unchanged, this suggests that either

the Ce ions did not enter into the lattices or did not change the average lattice spacing where they did enter. This evidence is similar to the work done by Kwon *et al.* [12].

The density and shrinkage values versus doping concentration of Ce and Cs are shown in the inset of Fig.2. The general trend indicates that doping slightly increased the density and shrinkage value. However, the Ce doped samples showed a higher increase. This result indicates that Ce doping helped to improve the densification of the doped CCTO ceramics. The microstructures of the doped samples are shown in Fig.3. For the Cs doping, average grain size increased from $\sim 20.4 \mu\text{m}$ for unmodified CCTO (Fig.3 (a)) to $\sim 28.9 \mu\text{m}$ for the 2.0mol% sample (Fig.3 (b)). In contrast to the Ce doping, a notable decrease in grain size was observed where the 2.0 mol% Ce sample had an average grain size of only $1.9 \mu\text{m}$ (Fig.3 (c)). This result implies that Cs doping promoted grain growth, while Ce doping inhibited grain growth. Furthermore, the reduced grain growth seen with the Ce ions gave rise to a segregation of the doping oxide which formed small scale secondary phases at the grain boundaries without being detected by XRD [10].

Plots of the dielectric properties as a function of temperature (Fig. 4 (a)) for the pure CCTO ceramic (100 Hz - 500 kHz) illustrated a high dielectric constant with temperature stability over the temperature range of $\sim 27\text{-}60^\circ\text{C}$ of the pure CCTO ceramics, while a tangent loss was less than 0.01 over a range of $27\text{-}70^\circ\text{C}$ at 10 kHz (Fig. 5 (a)). The dielectric constants as a function of temperature of the Cs (Fig. 4 (b)) and Ce (Fig. 4 (c)) doped CCTO ceramics (100 Hz - 500 kHz), indicates that doping of Cs produced a weak of frequency dispersion of the dielectric constant, in contrast to that of the Ce doping where a strong of frequency dispersion was observed. However, all doping conditions exhibited a reduction in dielectric constant at room temperature. This reduction has been observed for many modified CCTO ceramics [9-11].

The values of the loss tangent ($\tan \delta$) as a function of temperature for the Cs and Ce doped CCTO ceramics are shown in Figs. 5 (b) and (c), respectively. The Ce samples showed a change of $\tan \delta$ about 150% (from 0.2 at 27°C to 0.5 at 70°C) at 1 kHz, while Cs samples exhibited temperature and frequency stability (2% change) over the same temperature range.

The dielectric constants versus frequency plots at room temperature for the Cs and Ce doped ceramics (Fig.6) show decreasing trend with frequency. Furthermore, a significant decrease in the dielectric constant was observed for the Ce samples comparing to that of the Cs samples. Plots of the loss tangent versus frequency of the pure CCTO ceramic (Fig. 6) at room temperature, show that the loss tangent decreased with increasing frequency up to 1 kHz and then increased with further increases in frequency. However, the additions significantly lowered the rise in loss tangent at high frequencies (>1 kHz), implying a reduced conductivity of the doped ceramics.

From the IBLC model [6,7], the CCTO system can be viewed as a circuit consisting of two parallel RC elements connected in series which represent the semiconducting bulk, grain and insulating grain boundary, and grain boundary capacitor. It has also been proposed that the apparent dielectric constant (ϵ'_r) can be related to the grain size (d) and the thickness of the grain boundary (barrier width, t) and internal dielectric constant of the grain boundary (ϵ_{gb}) using the following expression:[13]

$$\epsilon'_r = \epsilon_{gb} \left(\frac{d}{t} \right) \quad (1)$$

In the present work, the reason for the reduction of the dielectric constant of the doped samples are uncertain, but could be linked to the characteristics of the grain boundaries. According to Eq. (1) it is possible that the dielectric constant of the grain boundaries for the doped samples decreased after doping [13] which could cause a decrease in the dielectric constant. Further, it should be noted that the dielectric constant for the Ce

doped samples is lower than the Cs doped samples. This could also result from a decrease in grain size (see also Eq.(1)), as seen in Fig.3, where a sharp decrease in grain size was recorded for the Ce doped samples.

In the case of the loss tangent behavior of the present samples, the reduction of $\tan \delta$ could be correlated to changes in transport behavior, i.e. an increase in total resistivity of the grain boundaries [14] (which in turn depends on the value of grain boundary resistance) which results in a lowered loss tangent. However, further investigation using different techniques should be performed to clarify the evidence.

4. Conclusions

The properties of Ce and Cs doped CCTO ceramics were investigated for the first time. The pure and modified (CCTO) ceramics were prepared by a conventional solid-state reaction technique. The different dopant resulted in different grain sizes, where Cs doping promoted grain growth, while Ce doping inhibited grain growth. Although these dopants produced a reduction in the dielectric constant, the dielectric constant after doping was still high especially for Cs doping. The loss tangent performance of the Cs samples was found to improve independently with temperature and frequency. It was proposed that the change in the microstructures could be related to the changes in the dielectric properties.

Acknowledgements

This work was supported by Development and Promotion of Science and Technology Talents Project (DPST), Thailand, Faculty of Science and Graduate School Chiang Mai University, the Thailand Research Fund (TRF). We also wish to thank the National Research University Project under Thailand's Office of the Higher Education Commission (OHEC) for financial support.

References

- [1] M.A. Subramanian, D. Li, N. Duan, B.A. Reisner, and A. W. Sleight, High dielectric constant in $\text{ACu}_3\text{Ti}_4\text{O}_{12}$ and $\text{ACu}_3\text{Ti}_3\text{FeO}_{12}$ phases, *Journal of Solid State Chemistry* 151 (2000) 323-325.
- [2] A.P. Ramirez, M. A. Subramanian, M. Gardel, G. Blumberg, D. Li, T. Vogt, and S. M. Shapiro, Giant dielectric constant response in a copper-titanate, *Solid State Communications* 115 (2000) 217-220.
- [3] W. Si, E.M. Cruz, P.D. Johnson, P. W. Barnes, P. Woodward, and A. P. Ramirez, Epitaxial thin films of the giant-dielectric-constant material $\text{CaCu}_3\text{Ti}_4\text{O}_{12}$ grown by pulsed-laser deposition, *Applied Physics Letters* 81(2002) 2056.
- [4] Y. Lin, Y.B. Chen, T. Garret, S.W. Liu, C.L. Chen, L. Chen, R.P. Bontchev, A. Jacobson, J.C. Jiang, E.I. Meletis, J. Horwitz, H.D. Wu, Epitaxial growth of dielectric $\text{CaCu}_3\text{Ti}_4\text{O}_{12}$ thin films on (001) LaAlO_3 by pulsed laser deposition, *Applied Physics Letters* 81 (2002) 631.
- [5] P. Lunkenheimer, V. Bobnar, A.V. Pronin, A.I. Ritus, A.A. Volkov, A. Loidl, Origin of apparent colossal dielectric constants, *Physical Review B* 66 (2002) 052105.
- [6] D.C. Sinclair, T.B. Adams, F.D. Morrison, and A. R. West, $\text{CaCu}_3\text{Ti}_4\text{O}_{12}$: One-step internal barrier layer capacitor, *Applied Physics Letters* 80 (2002) 2153.
- [7] T.B. Adams, D.C. Sinclair, and A.R. West, Characterization of grain boundary impedances in fine- and coarse-grained $\text{CaCu}_3\text{Ti}_4\text{O}_{12}$ ceramics, *Advanced Materials* 14 (2002) 1321.
- [8] G.F. Vander Voort, A.M. Gokhale, Comments on Grain size measurements, *Scripta Materialia* 26 (1992) 1655.
- [9] R.D. Shannon, C.T. Prewitt, Revised values of effective ionic radii, *Acta Crystallographica Section B* 26 (1970) 1046-1048.

- [10] Chun-Hong Mu, Peng Liu, Ying He, Jian-Ping Zhou, Huai-Wu Zhang, An effective method to decrease dielectric loss of $\text{CaCu}_3\text{Ti}_4\text{O}_{12}$ ceramics, *Journal of Alloys and Compounds* 471 (2009) 137–141.
- [11] S.Y. Chung, S.I. Lee, J.H. Choi, S.Y. Choi, Initial cation stoichiometry and current-voltage behavior in Sc-doped calcium copper titanate, *Applied Physics Letters* 89
- [12] S. Kwon, C.-C. Huang, E.A. Patterson, D.P. Cann, The effect of Cr_2O_3 , Nb_2O_5 and ZrO_2 doping on the dielectric properties of $\text{CaCu}_3\text{Ti}_4\text{O}_{12}$, *Materials Letters* 62 (2008) 633–636.
- [13] F. Amaral, M.A. Valente, L.C. Costa, Dielectric properties of $\text{CaCu}_3\text{Ti}_4\text{O}_{12}$ (CCTO) doped with GeO_2 , *Journal of Non-Crystalline Solids* 356 (2010) 822–827.
- [14] L. Ni, X.M. Chen, X.Q. Liu and R.Z. Hou, Microstructure-dependent giant Dielectric response in $\text{CaCu}_3\text{Ti}_4\text{O}_{12}$ ceramics, *Solid State Communications* 139 (2006) 45–50.

Figure captions

Fig. 1 XRD patterns of pure and doped CCTO ceramics. Insets (a) and (b) show XRD peaks of (422) planes for Cs and Ce doped CCTO ceramics, respectively.

Fig. 2 Lattice constant of doped CCTO ceramics as a function of Cs and Ce Concentrations. Inset shows density and shrinkage of doped CCTO ceramics versus Cs and Ce concentrations.

Fig.3 Fracture surfaces of selected samples: (a) Cs 2.0 mol% doped CCTO and (b) Ce 2.0 mol% doped CCTO.

Fig.4 Dielectric constant as a function of temperature for the ceramics: (a) pure CCTO, (b) Cs 2.0mol% doped CCTO and (c) Ce 2.0 mol% doped CCTO.

Fig.5 Loss tangent as a function of temperature of the ceramics: (a) pure CCTO, (b) Cs 2.0mol% doped CCTO and (c) Ce 2.0 mol% doped CCTO.

Fig. 6 Dielectric constant as a function of frequency of the ceramics and the inset shows their loss tangent.

Fig. 1

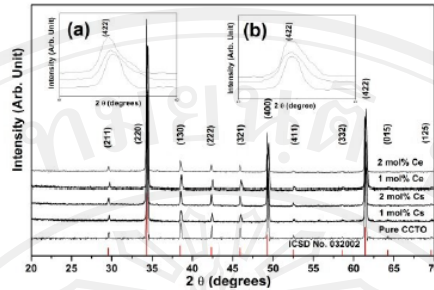
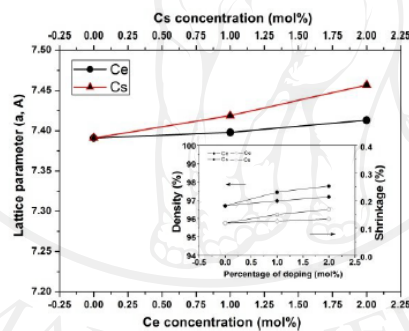


Fig. 2



ลิขสิทธิ์มหาวิทยาลัยเชียงใหม่
 Copyright© by Chiang Mai University
 All rights reserved

Fig. 3

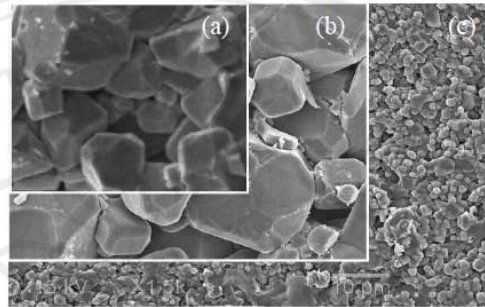


Fig. 4

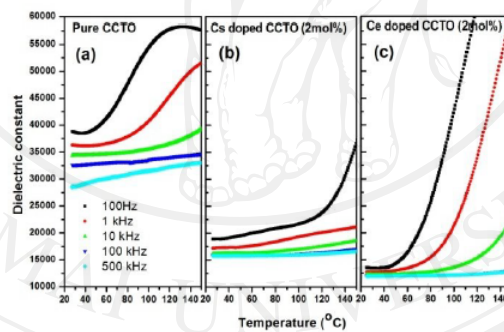


Fig.5

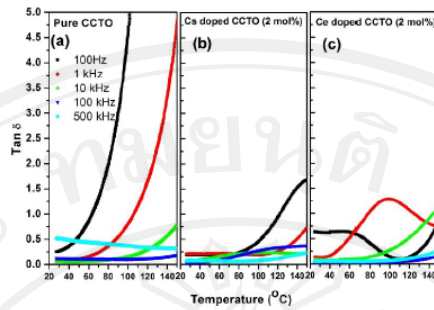


Fig. 6

